Multiphoton-Excited Fluorescence Imaging and Photochemical Modification of Dye-Doped Polystyrene Microsphere Arrays

Gerald H. Springer and Daniel A. Higgins*

Department of Chemistry, Kansas State University, Manhattan, Kansas 66506-3701

Received November 10, 1999. Revised Manuscript Received March 7, 2000

The use of nonlinear optical methods for thin-film polymeric materials modification and characterization is explored. Ordered 3-dimensional (3-D) dye-doped polystyrene microsphere arrays are photobleached and imaged in these studies. Efficient, irreversible photochemical bleaching of the dye within individual 0.5 and 1 μm diameter microspheres occurs when 810 nm light from a mode-locked Ti:sapphire laser is focused to an ~400 nm diameter spot within the spheres. Photobleaching is shown to result from three-photon absorption and may involve ionization of the dye. The three-photon-induced photochemistry is dramatically more efficient than that resulting from single-photon excitation. Imaging of the unbleached and bleached arrays is accomplished by monitoring the two-photon-excited fluorescence from the dye. Both the nonlinear photobleaching and imaging methods provide inherent depth-discriminating capabilities, allowing for high-resolution 3-D control of the volume modified and imaged. The results suggest that the methods and materials employed here may have important optical data storage applications. The capabilities of these methods are demonstrated by bleaching individual spheres in 3-D arrays, without affecting neighboring spheres. Optical data storage densities as high as 10^{13} bits/cm^3 are readily achievable. Unique photobleaching patterns observed within the spheres are explained by the radiation distribution within individual microspheres under focused-beam illumination.

I. Introduction

Ordered polymeric microsphere arrays find a range of possible applications in optical device technology. They are presently used in the fabrication of photonic band gap materials,[1] and may also have applications in organic light-emitting diodes.[2] The observation of stimulated emission[3] from novel whispering gallery modes has further increased interest in these materials.[4−8] Optical data storage in spheres and microsphere arrays has also recently been demonstrated. In previous work by Denk et al., it was shown that relatively large (6 μm diameter) dye-doped spheres could be locally photobleached and reimaged using multiphoton−excitation methods.[9] More recently, Kumacheva and co-workers demonstrated that conventional linear optical methods could be used in a similar manner to modify 3-D microsphere arrays.[10]

In this paper, it is demonstrated that well-ordered 3-D arrays of fluorescent microspheres may represent the best medium for microsphere-based data storage applications. In these arrays, individual spheres represent the individual bits. Because of the well-ordered nature of the arrays, the individual bits are inherently addressable (i.e., the location of each bit is defined by the physical position of the sphere). As originally demonstrated by Denk and co-workers,[9] it is also shown that multiphoton-based optical techniques are ideal for inducing photochemistry within the spheres and for imaging the 3-D sphere arrays (representing writing and readout steps in the data storage process). Similar methods have also recently been employed to fabricate microminiature devices in photoresist materials.[11,12]

Nonlinear optical methods provide several distinct advantages over alternative optical methods for materials modification and imaging.[13,14] Perhaps most importantly, the use of multiphoton absorption confines the volume modified to the volume of the laser focus.[9,11,12,15,16] The volume in which fluorescence is excited in imaging experiments is similarly confined, providing enhanced

* To whom correspondence should be addressed.

(1) Yablonovitch, E. *J. Mod. Opt.* **1994**, *41*, 173.
(2) Yamasaki, T.; Tsutsui, T. *Appl. Phys. Lett.* **1998**, *72*, 1957.
(3) Tzeng, H.; Wall, K. F.; Long, M. B.; Chang, R. K. *Opt. Lett.* **1984**, *9*, 499.
(4) Kuwata-Gonokami, M.; Takeda, K.; Yasuda, H.; Ema, K. *Jpn. J. Appl. Phys.* **1992**, *31 Pt. 2*, L99.
(5) Kuwata-Gonokami, M.; Takeda, K. *Opt. Mater.* **1998**, *9*, 12.
(6) Kamada, K.; Sasaki, K.; Masuhara, H. *Chem. Phys. Lett.* **1994**, *229*, 559.
(7) Fujiwara, H.; Sasaki, K.; Masuhara, H. *J. Appl. Phys.* **1999**, *85*, 2052.
(8) Sasaki, K.; Fujiwara, H.; Masuhara, H. *J. Vac. Sci. Technol. B* **1997**, *15*, 2786.
(9) Denk, W.; Strickler, J. H.; Webb, W. W. *Science* **1990**, *248*, 73.
(10) Kumacheva, E.; Kalinina, O.; Lilge, L. *Adv. Mater.* **1999**, *11*, 231.
(11) Cumpston, B. H.; Ananthavel, S. P.; Barlow, S.; Dyer, D. L.; Ehrlich, J. E.; Erskine, L. L.; Heikal, A. A.; Kuebler, S. M.; Lee, I. Y. S.; McCord-Maughon, D.; Qin, J.; Rockel, H.; Rumi, M.; Wu, X.; Marder, S. R.; Perry, J. W. *Nature* **1999**, *398*, 51.
(12) Witzgall, G.; Vrijen, R.; Yablonovitch, E.; Doan, V.; Schwartz, B. J. *Opt. Lett.* **1998**, *23*, 1745.
(13) Rucker, M.; Vanoppen, P.; De Schryver, F. C.; Ter Horst, J. J.; Hotta, J.; Masuhara, H. *Macromolecules* **1995**, *28*, 7530.
(14) Wedekind, P.; Kubitscheck, U.; Peters, R. *J. Microsc.* **1994**, *176*, 23.

10.1021/cm9907256 CCC: $19.00
Published on Web 04/14/2000

depth-discriminating abilities required for data storage in 3-D arrays. In addition to volume confinement, nonlinear excitation can lead to greatly enhanced photochemistry,[9,11,16] allowing for much more rapid materials modification. For imaging, the background-free nature of the signal (i.e., there are negligible contributions from Rayleigh and Raman scattering[17,18]) allows for the lowest possible light levels to be used, limiting further degradation and allowing for increased imaging (i.e., readout) rates. The use of a conventional light microscope for focusing the incident laser light to an ~400 nm diameter diffraction-limited spot size, coupled with the confinement effects described above, allows for the smallest possible microspheres (500 nm to 1 μm diameters) to be employed. Potential data storage densities of greater than 10^8 bits/cm^2 in 2-D arrays or 10^{13} bits/cm^3 in 3-D arrays can then be achieved.

II. Experimental Procedures

Microsphere arrays were prepared in thin films by spin casting an aqueous suspension of dye-doped 0.5 or 1 μm diameter polystyrene microspheres (Molecular Probes) onto a microscope coverslip. Evaporation of the water during spin casting resulted in the formation of large domains of hexagonally close-packed microspheres. These microspheres contained a dipyrromethene boron difluoride dye which has one-photon absorption and emission maxima at 540 and 560 nm, respectively.[19] Both the dye and the polymer absorb strongly in the UV as well.

Nonlinear absorption for both modification and imaging was induced in the sample by focusing the near-infrared (810 nm) pulses of light from a Ti:sapphire laser[20] to a submicrometer spot size in the spheres. The output of the laser was used directly (~80 MHz repetition rate). The excitation beam was passed through a visible blocking filter, a polarizer, and a halfwave plate, prior to being directed into an inverted light microscope (Nikon). A harmonic beam splitter was used to reflect the excitation beam into a high numerical aperture oil immersion objective. The objective was used to produce a nearly diffraction-limited focus in the sample (~400 nm diameter) and to collect the fluorescence emitted by the sample. High incident powers were used to bleach the spheres, while much lower powers were used for imaging. The excitation power for imaging experiments was always maintained at a level low enough to avoid photodestruction of the dye contained in the spheres; typically, average powers below 0.1 mW (at 80 MHz) were employed. To induce dye photochemistry, incident powers greater than ~5 mW were used.

In imaging experiments, residual 810 nm light was removed by passing the collected fluorescence back through the harmonic beam splitter and through a 650 nm short-pass filter. A single-photon counting photomultiplier tube (Hamamatsu, HC135-01), which is essentially blind to the excitation light was used to detect the emitted fluorescence. Fluorescence spectra were recorded by directing the emission through a spectrograph (Acton Research) and detecting it with a liquid-N_2-cooled CCD detector (Princeton Instruments). For imaging experiments, the sample was raster-scanned above the microscope objective, using a piezoelectrically driven scanning stage. The 514 nm output of an air-cooled argon ion laser was used (along with the appropriate filters) in some experiments for comparison of the two-photon excited fluorescence with that obtained from single-photon excitation.

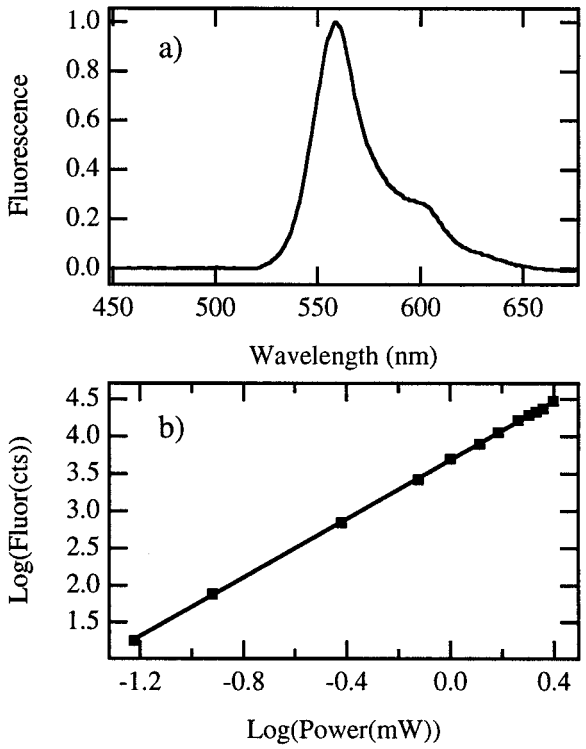

Figure 1. (a) Two-photon-excited fluorescence spectrum recorded for 1 μm diameter dye-doped polystyrene spheres. The spectrum shown was excited at 810 nm and is indistinguishable from that recorded by one-photon excitation at 514 nm. (b) Dependence of the observed fluorescence count rate (in 40 ms) on the power of incident 810 nm light. The log−log plot shows a linear dependence with a slope of 1.97, indicating two photons are being absorbed simultaneously by the dye.

III. Results and Discussion

With less than 0.1 mW of 810 nm light from the mode-locked Ti:sapphire laser incident through the microscope objective on a sample of dye-doped polystyrene microspheres, red/orange fluorescence is observed. The fluorescence spectrum recorded with excitation at 810 nm is shown in Figure 1a. With the laser operating in continuous-wave (CW) mode, no fluorescence is observed, indicating that it arises from a nonlinear excitation process. Proof that excitation occurs by the simultaneous absorption of two photons at 810 nm is obtained by measuring the power dependence of the fluorescence.[21] The plot shown in Figure 1b presents these results, which were recorded by using a polarizer/halfwave plate combination to vary the incident power. The data show a linear dependence of the log of the fluorescence count rate on the log of the incident power. A fit to the data yields a slope of 1.97, approximately what is expected for two-photon excitation in which the excitation rate depends on the square of the incident intensity.[9,21]

Figure 2a shows a fluorescence image of a dye-doped polystyrene microsphere (0.5 μm diameter) array imaged by detecting the two-photon-excited fluorescence. Regions such as those shown in Figure 2 are often well ordered, showing a hexagonal close-packed configura-

(15) Stelzer, E. H. K.; Hell, S.; Lindek, S.; Stricker, R.; Pick, R.; Storz, C.; Ritter, G.; Salmon, N. *Opt. Commun.* **1994**, *104*, 223.
(16) Shear, J. B. *Anal. Chem.* **1999**, *71*, 598 A.
(17) Xu, C.; Zipfel, W.; Shear, J. B.; Williams, R. M.; Webb, W. W. *Proc. Natl. Acad. Sci. U.S.A.* **1996**, *93*, 10763.
(18) Xu, C.; Shear, J. B.; Webb, W. W. *Anal. Chem.* **1997**, *69*, 1285.
(19) Haughland, P. U.S. Patent 5,326,692.
(20) Fisher, W. G.; Wachter, E. A.; Armas, M.; Seaton, C. *Appl. Spectrosc.* **1997**, *51*, 218.
(21) Friedrich, D. M. *J. Chem. Educ.* **1982**, *59*, 472.

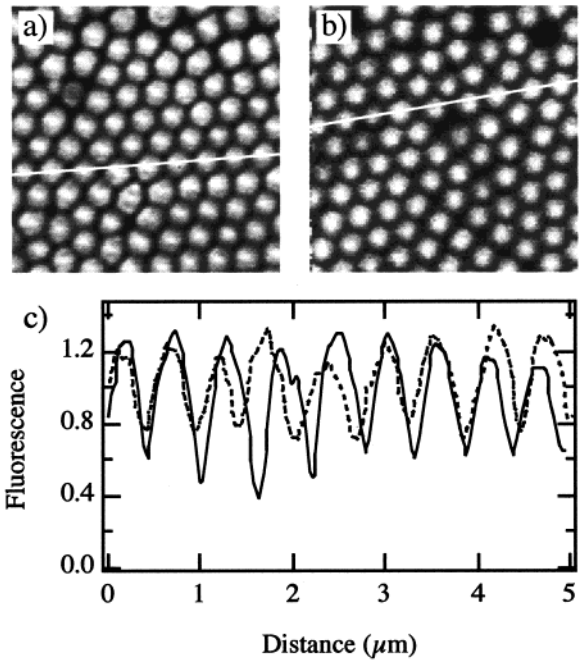

Figure 2. (a) Two-photon-excited fluorescence image of 500 nm dye-doped microspheres forming a regular, hexagonal array on a glass coverslip. Light at 810 nm was used to excite the dye. (b) Fluorescence image of a similar sample region excited by one-photon absorption at 514 nm. (c) Fluorescence line scans taken from the data in a and b, as designated by the white lines superimposed on the images. The solid line depicts the fluorescence recorded by two-photon excitation and the dashed line that observed for one-photon excitation. The two line scans demonstrate the similar contrast and resolution of the two excitation methods.

tion. However, larger scan sizes show that the film organization is somewhat less uniform, consisting of numerous ordered monolayer, and sometimes multilayered domains. Domain boundaries and missing sphere defects are routinely observed.[22,23] The appearance of these different film features is both a function of the method of film preparation and also of the processes involved in spontaneous organization of the microspheres.[24,25]

To evaluate the capabilities of two-photon excited fluorescence microscopy for high-resolution data storage applications, its imaging capabilities are first compared to one-photon excitation methods. Figure 2b presents images of a sphere array recorded using one photon CW excitation at 514 nm. Line scans of the fluorescence signal observed by the two methods are plotted in Figure 2c. Qualitatively, there appears to be little difference in both the resolution and contrast provided by the two methods. Denk et al. have come to similar conclusions in studies of other materials.[26] More quantitatively, this is indeed the result expected from well-known theories of optical imaging.[27] Briefly, for all forms of linear microscopy, the ultimate spatial resolution is given by[28]

$$\Delta x = \frac{0.61\lambda}{\mathrm{NA}} \tag{1}$$

where NA is the numerical aperture of the objective. If a Gaussian beam profile is assumed, the diffraction-limited resolution obtained using nonlinear optical methods scales approximately as $\Delta x/(n^{1/2})$, where n is the order of the process. With two-photon excitation at $\lambda = 810$ nm and NA = 1.3, resolution on the order of 270 nm is expected. One-photon excitation at 514 nm yields an expected resolution of 240 nm. Therefore, little is lost in terms of lateral resolution when two-photon methods are employed, while higher order processes are in fact expected to provide improved resolution.[29]

One of the main advantages of multiphoton excitation for materials modification/characterization and associated data storage applications is its inherent depth discriminating abilities. Again, it is well-known that the excitation volume is confined along the beam axis to the focal region by the nonlinear dependence on excitation intensity.[9,15] In contrast, for a uniform sample, fluorescence signals excited by one-photon absorption are independent of focus. As a result, improved image contrast may be expected in nonlinear imaging applications because signals from out-of-focus regions are effectively eliminated. As shown in the line scans presented in Figure 2c, the contrast in the two-photon-excited sphere image appears to be slightly better, consistent with these expectations. Hell et al. in a detailed study of one-photon microscopic methods have concluded that contrast is also enhanced simply by the use of femtosecond pulsed laser sources for imaging, in comparison to CW methods.[30]

Another important advantage of multiphoton methods is that more diverse and potentially more efficient photochemical processes can be used for materials modification.[11,12,16] Again, because of the depth discriminating abilities of these methods, such modifications are also more readily controlled and confined to specific volumes. The dye within the spheres studied here has been found to undergo very efficient photochemical bleaching at powers much above 1 mW, using pulsed 810 nm light. At relatively high incident powers (i.e., >20 mW), sphere fluorescence is reduced to 1/e of its initial value in about 1 s. At similar time-averaged excitation rates using 514 nm light (one-photon CW excitation), negligible bleaching is observed over much longer time scales. These results suggest that the bleaching process involves nonlinear excitation of the dye.

Figure 3a shows the results of multiphoton-induced photobleaching in a 1 μm sphere array. For this image, a 5 μm area has been photobleached by imaging the area at high excitation powers (once at 3.6 mW and a second time at 6.2 mW). The scan area was then increased, the incident power reduced, and the area reimaged. Clearly, the photobleaching process is highly localized, as evidenced by the spheres along the upper edge of the

(22) Dimitrov, A. S.; Nagayama, K. *Chem. Phys. Lett.* **1995**, *243*, 462.
(23) Wang, Y.; Juhue, D.; Winnik, M. A.; Leung, O.; Goh, M. C. *Langmuir* **1992**, *8*, 760.
(24) Dimitrov, A. S.; Nagayama, K. *Langmuir* **1996**, *12*, 1303.
(25) Dushkin, C. D.; Nagayama, K.; Miwa, T.; Kralchevsky, P. A. *Langmuir* **1993**, *9*, 3695.
(26) Denk, W.; Piston, D. W.; Webb, W. W. Two-Photon Molecular Excitation in Laser-Scanning Microscopy. In *Handbook of Biological Confocal Microscopy*; Pawley, J. B., Ed.; Plenum Press: New York, 1995; p 445.
(27) Wilson, T.; Sheppard, C. *Theory and Practice of Scanning Optical Microscopy*; Academic Press: Orlando, 1984.
(28) Abbe, E. *Archiv. Mikros. Anat.* **1873**, *9*, 413.
(29) Nakamura, O. *Optik* **1993**, *93*, 39.
(30) Hell, S. W.; Hanninen, P. E.; Salo, J.; Kuusisto, A.; Soini, E.; Wilson, T.; Tan, J. B. *Opt. Commun.* **1994**, *113*, 144.

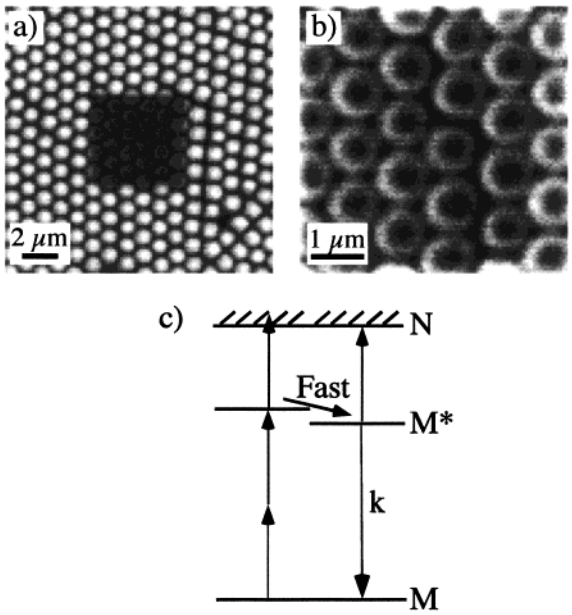

Figure 3. (a) Two-photon-excited fluorescence image of 1 μm diameter spheres showing a previously photobleached region of the film. (b) An image recorded by zooming in on the photobleached region in a. Fluorescent "rings" are observed for partially photobleached spheres. (c) Model for the energy levels of the dye dopant and the relevant excitation, emission, and photobleaching processes.

bleached region. Only the lower hemispheres (in the image plane) have been bleached. Sequentially recorded images prove that the photobleaching process is irreversible and that the dye molecules have limited mobility in these solid spheres. No evidence of recovery after photobleaching is observed on any time scale.[31−33]

Conclusive evidence for the higher-order nature of the induced photochemistry can be obtained by measuring the power dependence of the rate of photobleaching. As discussed below, it is believed bleaching occurs via three-photon absorption by the dye. Using rate expressions generalized from previous publications[16,21] for the model shown in Figure 3c, the relationship between incident intensity and bleaching rate can be predicted. In Figure 3c, M, M*, and N represent the relaxed, excited, and photodecomposed dye molecule, respectively. The excited state denoted by M* is certainly different from that initially prepared by two-photon excitation. Such a conclusion may be drawn from experimental spectral data, Kasha's Rule, and also from symmetry arguments.[34] The initially prepared excited state relaxes very rapidly to M* and is therefore neglected in the model. The rate of production of bleached product, N, assuming three-photon excitation is given by

$$\frac{d[N]}{dt} = \delta' I^3[M] + \sigma I[M^*] \qquad (2)$$

where δ' represents the three-photon-absorption cross section of the dye, σ represents the one-photon-absorption cross section for the excited dye molecule, and I is the incident intensity. Note that eq 2 includes both the possibility for direct three-photon-induced decomposition of the dye as well as that occurring via one-photon excited-state absorption. Equation 2 can be generalized to describe higher order processes by simply replacing the intensity terms and absorption cross sections with their appropriate counterparts.

Excitation to M* and subsequent emission from this state are assumed to be very fast in comparison to the bleaching process. Therefore, the relative populations of M and M* may be found from steady-state expressions and is given by

$$[M^*] = \frac{\delta I^2}{k}[M] \qquad (3)$$

where δ is the two-photon absorption cross section for the ground-state dye and k is the rate constant for emission from M*. By using the appropriate mass-balance expression relating concentrations of all species to the total dye concentration $[M_o]$, it can then be shown that the rate of production of N is given by

$$\frac{[N]}{[M_o]} = 1 - \exp\left(\frac{-t}{1 + \delta I^2/k}\left(\delta' + \frac{\sigma\delta}{k}\right)I^3\right) \qquad (4)$$

From eq 4, it is clear that the signal decay rate (due to photobleaching) should exhibit a complex dependence on excitation intensity. At low powers, the decay rate should scale as I^3, regardless of the exact nature of bleaching (i.e., direct or via the initial formation of M*). At higher powers, where significant population of M* occurs (i.e., when $\delta I^2/k$ approaches unity), the bleaching kinetics become linearly dependent on incident intensity.

Power-dependent studies of the bleaching kinetics show multiexponential decays in the fluorescence signal. Figure 4a shows data from a typical experiment at an incident power of 18 mW. The decay shown was fit to a double exponential, yielding fast and slow decay constants of 0.64 and 0.11 s^{-1}, respectively. Fits to data recorded for a range of powers show the fast time component varies as expected with I^3 at powers <25 mW. Figure 4b shows a log−log plot of decay rate vs incident power. A linear fit to these data yields a slope of 2.6, demonstrating that the process likely results from absorption of three photons. These results vary somewhat between individual experiments because of the highly nonlinear nature of the excitation process and slight variations in experimental conditions (i.e., the focal position within the spheres). An average slope of 3.0 ± 0.8 was determined from several repetitions of the experiment.

At higher powers (>25 mW), the decay kinetics show a weaker dependence on incident intensity (not shown). Approximate predictions of the power-dependent decay kinetics using eq 4 and assumed cross sections indicate that the transition from an I^3 to I dependence may

(31) Blonk, J. C. G.; Van Aalst, D. H.; Birmingham, J. J. *J. Microsc.* **1993**, *169*, 363.

(32) Koppel, D. E. Fluorescence photobleaching as probe of translational and rotational motions. In *Fast Methods in Physical Biochemistry and Cell Biology*; Sha'afi, R. I., Fernandez, S. M., Eds.; Elsevier Science Publishers: New York, 1983; p 339.

(33) Kubitscheck, U.; Wedegind, P.; Peters, R. *J. Microsc.* **1998**, *192*, 126.

(34) Wirth, M. J.; Koskelo, A.; Sanders, M. J. *Appl. Spectrosc.* **1981**, *35*, 14.

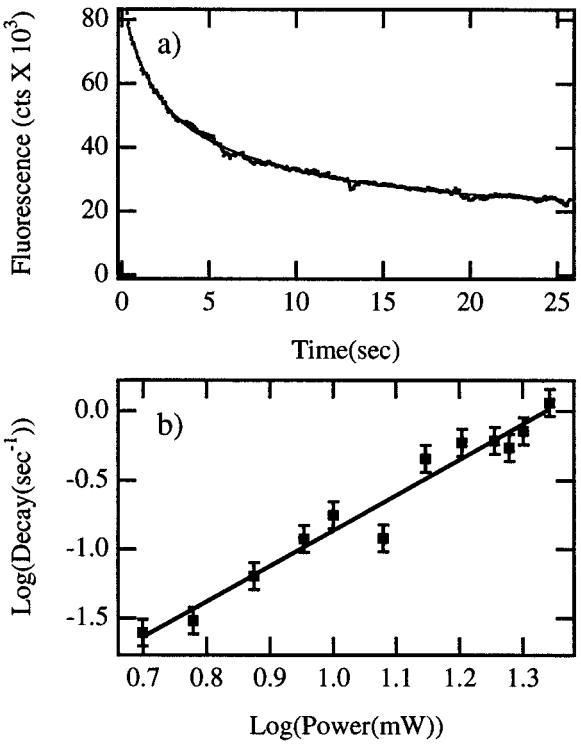

Figure 4. (a) Bleaching kinetics for a single sphere, recorded at an incident power of 18 mW. The decay of the two-photon excited fluorescence is plotted as a function of time. A double exponential was used to fit the data. (b) Dependence of the fast component of the fluorescence decay on the incident power. The log−log plot shows a linear dependence of the bleaching rate on incident power. A linear fit to the data yields a slope of 2.6. Results from several experiments yield an average slope of 3.0 ± 0.8, indicating the photochemistry is induced by three-photon absorption in the dye-doped spheres.

indeed occur near the intensities employed. It is believed that multiphoton absorption by the polymer matrix and possibly by the bleaching products may contribute to the complexity of the decay kinetics. Likewise, other optical phenomena such as self-focusing may also be important. However, the results shown in Figure 4 are consistent with three-photon-induced photobleaching. It is therefore proposed that photobleaching occurs via three-photon-induced ionization and subsequent decomposition of the dye, rather than via chemistry (i.e., reaction with oxygen) occurring from the fluorescent excited state (M*) itself. Photodecomposition from a triplet state of the dye produced by intersystem crossing from M* may also be ruled out.

Figure 3b shows that the bleached spheres yield a ring-shaped fluorescence pattern when reimaged. Most extensive photobleaching occurs at the center of each sphere. While such a pattern could be produced by a nonuniform distribution of dye (i.e., if the dye is concentrated in outer circumferential regions), the manufacturer indicates the spheres are uniformly doped. In addition, this pattern is not observed in images of unbleached spheres at any focus depth. Therefore, it is concluded that the spheres are indeed uniformly doped and the pattern results from the photobleaching process. This same bleaching pattern has also been observed in near-field optical bleaching and imaging studies of coumarin-doped microspheres embedded in a poly(vinyl alcohol) matrix.[13] In this previous work, the authors attributed the nonuniform bleaching to the overlap of

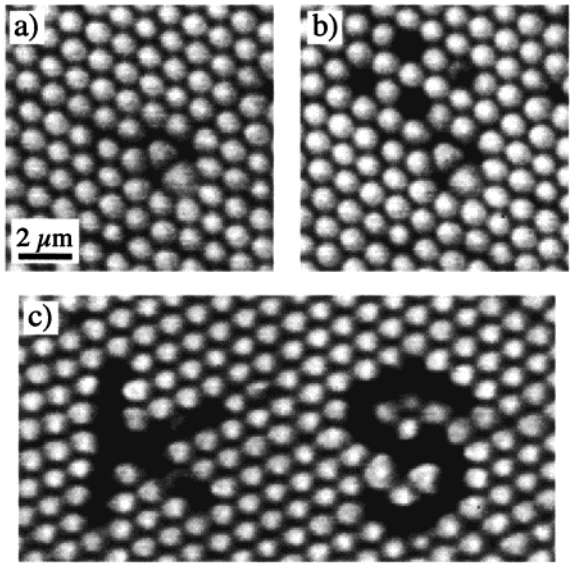

Figure 5. (a) An unbleached region of an ordered 1 μm sphere array that was subsequently reimaged, as shown in b, after four single spheres in the upper portion of the image had been partially photobleached. (c) Letters written in the film by selectively photobleaching single spheres. These data demonstrate the potential applications of sphere arrays in 2-D optical data storage applications.

the radiation field in the near-field experiments with the isotropic distribution of dye in the microspheres.

In the present work, it is proposed that nonuniform bleaching results from variations in the radiation-coupling efficiency and intensity profiles produced within the individual spheres as they are scanned over the focused laser spot. Radiation focusing within the sphere results from refraction at the sphere surface, as well as by multiple internal reflections within the spheres,[35−38] producing a much greater intensity at points along the central sphere axis (parallel to the direction of beam propagation).[39,40] From this model, photobleaching is indeed expected to be most extensive in the center of the sphere, as observed (see Figure 3). This phenomenon is further enhanced by the nonlinear methods employed here, resulting in more dramatic spatial confinement of bleaching.

The photobleaching methods presented here can be readily used for 2-D optical data storage. The images presented in Figure 5 demonstrate such an application. In Figure 5, several individual spheres have been selectively photobleached, while not damaging any of the surrounding spheres. Bleaching of the spheres was accomplished by first locating the spheres by imaging the area shown at low incident powers. The single spheres were then individually selected and moved into the focused laser spot. Powers up to 25 mW were used to almost completely bleach the spheres in a few seconds. While such rates are too slow for practical data storage applications, it may be possible to design dyes

(35) Astaf'eva, L. G.; Ledneva, G. P. *High Temp.* **1997**, *35*, 451.
(36) Barton, J. P.; Alexander, D. R.; Schaub, S. A. *J. Appl. Phys.* **1988**, *64*, 1632.
(37) Barton, J. P.; Alexander, D. R.; Schaub, S. A. *J. Appl. Phys.* **1989**, *65*, 2900.
(38) Saloma, C.; Cambaliza, M. O. *Appl. Opt.* **1995**, *34*, 3522.
(39) Lai, H. M.; Leung, P. T.; Poon, K. L.; Young, K. *J. Opt. Soc. Am. A.* **1991**, *8*, 1553.
(40) Dusel, P. W.; Kerker, M.; Cooke, D. D. *J. Opt. Soc. Am.* **1979**, *69*, 55.

that are much more photochemically active following multiphoton excitation, thereby greatly increasing the bleaching rate. Despite the present limitations, the advantages provided by microsphere arrays and the nonlinear optical methods employed here suggest such methods may warrant further investigation.

At higher laser powers, the spheres can actually be melted, possibly presenting an alternative mechanism for materials modification. Simultaneous absorption of several IR photons can lead to heating of the polymer above its glass transition temperature (T = 363 K).[41] Optical imaging experiments do not conclusively prove whether the spheres have been melted. However, topographic images recorded in a near-field optical microscope prove that such is indeed the case when high powers are employed. At even higher powers, the spheres may actually be ablated from the substrate surface.[42−46] While such processes are much more rapid than photobleaching, they are also less easily controlled, often leading to damage of surrounding spheres. It is therefore believed that the photobleaching methods are potentially most useful.

As noted above, because of the nonlinear nature (three-photon absorption) of the photobleaching process, the volume photobleached can be controlled in 3-D. This process can therefore be used for 3-D data storage in 3-D microsphere arrays, as has been demonstrated previously for uniform photobleachable polymer films,[47] and for microspheres.[9] Three-dimensional control of the photobleaching process is demonstrated in the images presented in Figure 6. Imaged in Figures 6a−c is a step region comprised of two ordered layers of microspheres. Figure 6a shows the two-photon-excited fluorescence image of the lower layer, while Figure 6b shows a similar image of the upper layer (found only on the right side of the image). Figure 6c shows an image recorded at intermediate focus. The positions of the spheres in Figures 6a,b have been highlighted, as have their positions in Figure 6c, depicting their registry. Parts d and e of Figure 6 demonstrate that single spheres within the individual layers can be selectively photobleached. As in the case of the 2-D arrays, surrounding spheres (in 3-D) are left undamaged. These images clearly demonstrate that these methods may therefore be useful in 3-D optical data storage applications.

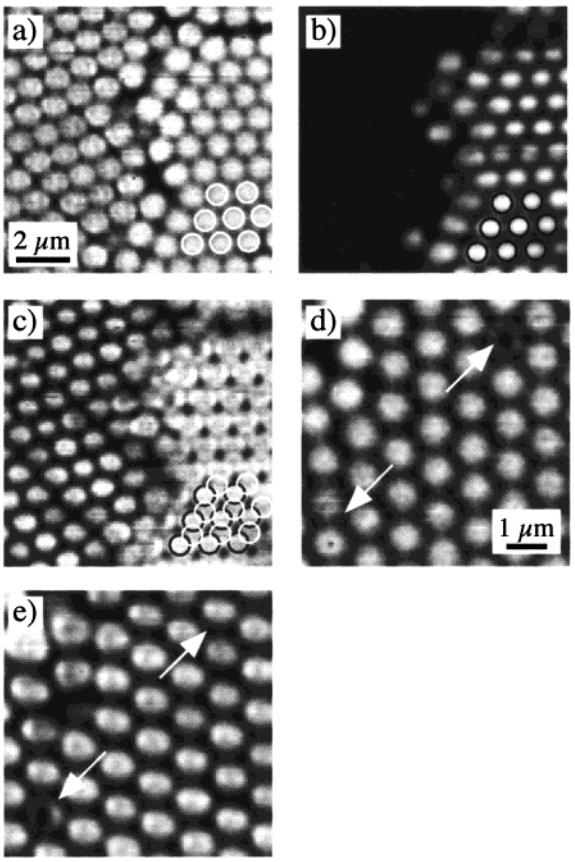

Figure 6. (a) Two-photon-excited fluorescence image of a two layer region of ordered spheres. The image shows the lower layer of spheres closest to the substrate. (b) The upper layer of spheres in the same region imaged in a. (c) An image recorded at intermediate focus, showing the blending of the images of both layers. These results demonstrate the inherent depth discrimination capabilities of two-photon excitation methods. (d and e) The lower and upper, respectively, sphere layers with a single sphere selectively removed from each by photobleaching. The arrows designate the location of the bleached sphere in each layer. These images demonstrate the possibility for 3-D data storage and optical device fabrication in 3-D ordered sphere arrays.

IV. Conclusions

Two-photon-excited fluorescence microscopy and mulitiphoton-induced photochemistry were shown to be valuable methods for both characterization and modification of dye-doped polymeric microsphere arrays. Multiphoton-induced photobleaching of the dye dopant was used to alter the fluorescence properties of individual microspheres. Two-photon-excited fluorescence imaging was then used to reimage the modified arrays. These images conclusively show that individual spheres could be bleached without affecting neighboring spheres. The nature of the photobleaching mechanism was studied to determine the order of the associated nonlinear excitation process. The results indicate the photobleaching mechanism involves three-photon excitation of the dye. Spatial variations in the intensity of light within the spheres, resulting from internal reflections within the spheres and refraction at the sphere surface were suggested to be the primary cause of the observed spatial variations in the extent of photobleaching. The use of these phenomena for optical data storage was proposed. The possibility for permanent optical data storage in 2- and 3-D microsphere arrays was demonstrated.

Acknowledgment. The work described herein was supported by the National Science Foundation under grants CHE-9701509 and CHE-9709034. Kansas State University and 3M Corporation are also acknowledged for their contributions. Erwen Mei and Angela M. Bardo, both of Kansas State University, are thanked for their help in collecting data.

CM9907256

(41) Reding, F. P.; Faucher, J. A.; Whitman, R. D. *J. Polym. Sci.* **1962**, *57*, 483.
(42) Yeh, J. T. C. *J. Vacuum Sci. Technol. A* **1986**, *4*, 653.
(43) Geertsen, C.; Briand, A.; Chartier, F.; Lacour, J.; Mauchien, P.; Sjostrom, S.; Mermet, J. *J. Anal. Atomic Spectrosc.* **1994**, *9*, 17.
(44) Srinivasan, R. *Appl. Phys. A* **1993**, *56*, 417.
(45) Srinivasan, R. *J. Appl. Phys.* **1993**, *73*, 2743.
(46) Catry, C.; Jeuris, K.; Jackers, C.; Hofkens, J.; Bastin, L.; Gensch, T.; Grim, P. C. M.; De Schryver, F. C. *Langmuir* **1999**, *15*, 1364.
(47) Gu, M.; Day, D. *Opt. Lett.* **1999**, *24*, 288.